ORIGINAL RESEARCH ARTICLE

WILEY | Journal of Cellular Physiology

Maduramicin induces cardiac muscle cell death by the ROS-dependent PTEN/Akt–Erk1/2 signaling pathway

Xin Chen[1,2,4] | Yue Li[1] | Meng Feng[1] | Xiaoyu Hu[1] | Hai Zhang[1] | Ruijie Zhang[1] | Xiaoqing Dong[1] | Chunxiao Liu[1] | Zhao Zhang[1] | Shanxiang Jiang[4] | Shile Huang[2,3] | Long Chen[1]

[1]Jiangsu Key Laboratory for Molecular and Medical Biotechnology, College of Life Sciences, Nanjing Normal University, Nanjing, China

[2]Department of Biochemistry and Molecular Biology, Louisiana State University Health Sciences Center, Shreveport, Louisiana

[3]Feist-Weiller Cancer Center, Louisiana State University Health Sciences Center, Shreveport, Louisiana

[4]Laboratory of Veterinary Pharmacology and Toxicology, College of Veterinary Medicine, Nanjing Agricultural University, Nanjing, China

Correspondence
Long Chen, Ph.D., Jiangsu Key Laboratory for Molecular and Medical Biotechnology, College of Life Sciences, Nanjing Normal University, 1 Wenyuan Road, Chixia District, 210023 Nanjing, Jiangsu, China.
Email: lchen@njnu.edu.cn
Shile Huang, Ph.D., Department of Biochemistry and Molecular Biology, Louisiana State University Health Sciences Center, 1501 Kings Highway, Shreveport, LA 71130-3932.
Email: shuan1@lsuhsc.edu

Abstract

Maduramicin (Mad), a polyether ionophore antibiotic, has been reported to be toxic to animals and humans because of being used at high doses or for long time, resulting in heart failure. However, the toxic mechanism of Mad in cardiac muscle cells is not well understood. Here, we show that Mad induced cell viability reduction and apoptosis in cardiac-derived H9c2, HL-1 cells, primary cardiomyocytes, and murine cardiac muscles, which was because of the inhibition of extracellular-signal-regulated kinase 1/2 (Erk1/2). Expression of constitutively active mitogen-activated protein kinase kinase 1 (MKK1) attenuated Mad-induced cell death in H9c2 cells, whereas silencing Erk1/2 or ectopic expression of dominant negative MKK1 strengthened Mad-induced cell death. Moreover, we found that both phosphatase and tensin homolog on chromosome 10 (PTEN) and protein kinase B (Akt) were implicated in the regulation of Erk1/2 inactivation and apoptosis in the cells and tissues exposed to Mad. Overexpression of dominant negative PTEN and/or constitutively active Akt, or constitutively active Akt and/or constitutively active MKK1 rescued the cells from Mad-induced dephosphorylated-Erk1/2 and cell death. Furthermore, Mad-induced reactive oxygen species (ROS) activated PTEN and inactivated Akt–Erk1/2 contributing to cell death, as N-acetyl-L-cysteine ameliorated the event. Taken together, the results disclose that Mad inhibits Erk1/2 via ROS-dependent activation of PTEN and inactivation of Akt, leading to cell death in cardiac muscle cells. Our findings suggest that manipulation of the ROS–PTEN–Akt–Erk1/2 pathway may be a potential approach to prevent Mad-induced cardiotoxicity.

KEYWORDS
Akt, apoptosis, cardiac muscle cells, maduramicin, PTEN, ROS

1 | INTRODUCTION

Maduramicin (Mad), a most potent polyether ionophore antibiotic for coccidiosis prevention, is used as a feed additive at 5–7 ppm (mg/kg) with a withdrawal period of 5 days before slaughter in chickens and turkeys for fattening (Dorne et al., 2013). Many reports have documented that Mad is toxic to animals and humans if improperly used (Bastianello, Fourie, Prozesky, Nel, & Kellermann, 1995; Dorne et al., 2013; Fourie, Bastianello, Prozesky, Nel, & Kellerman, 1991; Jayashree & Singhi, 2011; Shimshoni et al., 2014). Clinical data have shown that Mad evokes anorexia, diarrhea, dyspnea, depression, ataxia, recumbency, and death, and especially Mad results in degeneration and/or necrosis of heart and skeletal muscles (Bastianello et al., 1995; Dorne et al., 2013; Fourie et al., 1991; Jayashree & Singhi, 2011; Shimshoni et al., 2014). For example, Mad induces severe myocardial lesions in chickens, pigs, gilts, calves (Bastianello et al., 1995; Dorne et al., 2013; Fourie et al., 1991; Sanford & McNaughton, 1991; Shimshoni et al., 2014; Shlosberg et al., 1992, 1997; Singh & Gupta, 2003). Importantly, increasing cases of poisoning with Mad by accident have been reported in humans, especially in children, leading to rhabdomyolysis, acute renal failure, and even death (Jayashree & Singhi, 2011; Sharma, Bhalla, Varma, Jain, & Singh, 2005). Recently, we have demonstrated that Mad inhibits proliferation by arresting cells at G_0/G_1 phase of the cell cycle and induces caspase-dependent apoptosis in C2C12 myoblast cells (X. Chen et al., 2014). However, how Mad induces apoptotic cell death in cardiac muscle cells is not well understood.

Extracellular-signal-regulated kinase 1/2 (Erk1/2), a member of mitogen-activated protein kinases, plays a crucial role in the regulation of cell proliferation/growth and apoptosis (Kyriakis & Avruch, 2012; Xia, Liu, & Cheng, 2016). For example, Erk1/2 is involved in the doxorubicin-induced apoptosis in H9c2 cells and neonatal cardiomyocytes (Liu, Mao, Ding, & Liang, 2008). Sialyl-transferase 7A promotes cardiomyocyte apoptosis through the inhibition of Erk1/2 activity under hypoxic conditions (D. Zhang et al., 2015). Erk2 knockdown enhances caspase 3 activity in H_2O_2-stimulated neonatal rat cardiomyocytes (Ulm et al., 2014). Besides, it has been reported that monensin, another polyether ionophore antibiotic, increases the Erk1/2 activity in NCI-H929 myeloma cells (Park, Kim, Kim, & Lee, 2003). This prompted us to focus on studying whether Mad affects the Erk1/2 activity leading to apoptosis in cardiac muscle cells.

Phosphatase and tensin homolog on chromosome 10 (PTEN), a dual phosphatase which dephosphorylates proteins and phosphoinositides substrates, is an important negative regulator of Akt (Bermudez Brito, Goulielmaki, & Papakonstanti, 2015; Maehama & Dixon, 1999; Panigrahi et al., 2004). Interestingly, recent studies have shown that PTEN also negatively regulates the Erk1/2 pathway in several malignancies (Chetram & Hinton, 2012). In addition, Akt is able to activate Erk1/2 through protein kinase C (PKC) (Chetram & Hinton, 2012). Of note, multiple studies have documented that excessive reactive oxygen species (ROS)-induced cardiomyocyte apoptosis links to dysfunction of PTEN, Akt, and/or Erk1/2 signaling

(Kim, Kim, Shin, Kwon, & Park, 2014; Lv et al., 2014; Matsuno et al., 2012; Tian, Daoud, & Shang, 2012; Y. Yao et al., 2012; H. Yao et al., 2016). For example, H_2O_2 induces injury in cardiac myocytes via inhibiting PTEN protein expression (Lv et al., 2014). Doxorubicin induces injury through the PTEN/Akt and Erk pathway in H9c2 cells (Yao et al., 2016). Salinomycin, another polyether ionophore, induces intracellular ROS overproduction (Verdoodt et al., 2012; Zhou et al., 2013). Based on the above findings, we hypothesized that Mad may affect the Erk1/2 pathway via the ROS-mediated PTEN–Akt signaling pathway, thereby leading to cardiac apoptosis.

Here, for the first time, we show that Mad-induced ROS activates PTEN and inactivates Akt–Erk1/2, leading to apoptosis in cardiac muscle cells. Our findings underline that intervention in the ROS–PTEN–Akt–Erk1/2 signaling pathway may be a potential approach to prevent Mad-induced cardiotoxicity.

2 | MATERIALS AND METHODS

2.1 | Reagents

Mad ammonium was purchased from Santa Cruz Biotechnology (Santa Cruz, CA). 4′,6-Diamidino-2-phenylindole (DAPI), N-acetyl-L-cysteine (NAC) and 5-bromo-2-deoxyUridine (BrdU) were from Sigma (St. Louis, MO). Dulbecco's modified Eagle's medium (DMEM), Ham's F12 nutrient medium (F12), and 0.05% trypsin–EDTA were purchased from Invitrogen (Grand Island, NY), whereas Claycomb medium was provided by Sigma. Fetal bovine serum (FBS) was supplied by Hyclone (Logan, UT). CellTiter 96AQ$_{ueous}$ One Solution Cell Proliferation Assay kit was from Promega (Madison, WI). Annexin-V–fluorescein isothiocyanate (FITC)/propidium iodide (PI) Apoptosis Detection kit was purchased from BD Biosciences (San Diego, CA). 5-(and-6)-chloromethyl-2′,7′-dichlorodihydrofluorescein diacetate (CM-H$_2$DCFDA) was from MP Biomedicals (Solon, OH). Enhanced chemiluminescence reagent was from Millipore (Billerica, MA). Other chemicals were purchased from local commercial sources and were of analytical grade.

2.2 | Cell culture

Rat cardiac myoblast H9c2 cells (CRL-1446; American Type Culture Collection, Manassas, VA) were cultured in DMEM supplemented with 10% FBS, 4.5 mg/ml high glucose, 100 U/ml penicillin, 100 U/ml streptomycin, 2 mM L-glutamine. Murine cardiomyocytes HL-1 cells, a gift from William Claycomb (Louisiana State University Health Sciences Center, New Orleans, LA), were grown in Claycomb medium supplemented with 10% FBS, 100 μM norepinephrine, 100 U/ml penicillin, 100 U/ml streptomycin, and 2 mM L-glutamine (Sun et al., 2017). All cell lines were maintained in a humidified incubator containing 5% CO_2 at 37°C.

Primary cardiomyocytes were isolated from hearts of neonatal mice at 1–3 days old, as described previously (W. Zhang, Clair, Butterfield, & Vore, 2016). Briefly, neonatal institute of cancer research (ICR) mice were killed by cervical dislocation, and hearts

were removed with the ventricles only retained by a chest operation under sterile conditions, followed by washing with cold Ca^{2+}/Mg^{2+}-free Hank's balanced salt solution. Then, the ventricles were minced into small pieces and digested with 0.05% trypsin without Ca^{2+} and Mg^{2+}, with serial cycles of agitation. Subsequently, the supernatant containing the isolated cells was collected and FBS was added to a final concentration of 10%. The resulting mixture was centrifuged for 10 min at 100g, and the pelleted cells were then resuspended in DMEM/F12 (1:1) supplemented with 10% FBS. As nonmyocytes attach to the substrata more rapidly, to exclude nonmyocytes, the isolated cells were first seeded in 100-mm culture dishes. After 2-hr culture in a humid incubator (37°C, 5% CO_2), the nonattached cells were collected. Finally, the isolated cells were seeded at a 96-well plate (1×10^4 cells/well) or a 6-well plate (2×10^6 cells/well), supplemented with 100 μM BrdU during the first 48 hr to prevent the proliferation of nonmyocytes.

2.3 | Animals and administration with Mad

Thirty male ICR mice, weighing 18–22 g, were purchased from the Laboratory Animal Center, Nanjing Medical University (Nanjing, China). All animals were handled in accordance with the guidelines of the Institutional Animal Care and Use Committee and were in compliance with the guidelines set forth by the Guide for the Care and Use of Laboratory Animals. The mice were housed at room temperature (20–25°C), relative humidity of 60%, subjected to a 12-hr light/dark cycle under conventional barrier protection, and supplied with water and feed ad libitum. After acclimatization to these conditions for 1 week, the mice were randomly divided into normal control group and Mad treatment group (15 mice/group). A subacute Mad regimen (3.5 mg/kg), according to $1/10$ LD_{50}, was used. The mice in the Mad treatment group were intragastrically administered with Mad solution, which was dissolved in 2 ml of 100% ethanol and then diluted 10-fold with distilled water to obtain a final concentration of 0.2 mg/ml, and the control group received intragastric administration of water/vehicle daily for 7 days. At the end of the experiment, all animals were sacrificed by cervical dislocation, and heart tissues (retaining the ventricles only) were immediately removed and fixed in 4% paraformaldehyde or stored at −80°C for further analysis.

2.4 | Recombinant adenoviral constructs and infection of cells

Recombinant adenoviruses expressing green fluorescence protein (Ad-GFP), FLAG-tagged constitutively active mitogen-activated protein kinase kinase 1 (MKK1) (Ad-MKK1-R4F), FLAG-tagged dominant negative MKK1 (Ad-MKK1-K97M), and human dominant negative PTEN (Ad-PTEN-C/S) were described previously (Findley, Cudmore, Ahmed, & Kontos, 2007). Recombinant adenovirus expressing hemagglutinin (HA)-tagged constitutively active Akt (Ad-myr-Akt) was generously provided by Dr. Kenneth Walsh (Boston University, Boston, MA) (Fujio & Walsh, 1999). For experiments, cells were grown in the growth medium and infected with the individual adenovirus for 24 hr at 5 of multiplicity of infection. Subsequently, cells were used for

experiments. Ad-GFP served as a control. Expression of FLAG-tagged MKK1-R4F and MKK1-K97M and HA-tagged myr-Akt was determined by western blot analysis with antibodies to FLAG and HA, respectively.

2.5 | Lentiviral short hairpin RNA cloning, production, and infection

Lentiviral short hairpin RNAs (shRNAs) to Erk1/2 and GFP (for control) were constructed and infected as described previously (L. Chen, Liu, Luo, & Huang, 2008). For use, monolayer H9c2 cells, when grown to approximately 70% confluence, were infected with above lentivirus-containing supernatant in the presence of 8 μg/ml polybrene for 24 hr and exposed to 2 μg/ml puromycin for 48 hr. In 5 days, cells were used for experiments.

2.6 | Analysis for cell viability

H9c2 cells, HL-1 cells, and primary cardiomyocytes or H9c2 cells infected with Ad-MKK1-R4F, Ad-MKK1-K97M, Ad-PTEN-C/S, Ad-myr-Akt, Ad-PTEN-C/S/Ad-myr-Akt, Ad-myr-Akt/Ad-MKK1-R4F or Ad-GFP, or H9c2 cells infected with lentiviral shRNAs to Erk1/2 or GFP, respectively, were seeded in a 96-well plate (1×10^4 cells/well). Next day, cells were treated with 0–1 μM Mad or with/without 0.5 and 1 μM Mad for 48 hr or treated with/without 0.5 and/or 1 μM Mad for 48 hr after preincubation with/without 5 mM NAC for 1 hr with six replicates of each treatment. Subsequently, cell viability, after incubation with 3-(4,5-dimethylthiazol-2-yl)-5-(3-carboxy-methoxyphenyl)-2-(4-sulfophenyl)-2H-tetrazolium, inner salt (MTS) reagent (one solution reagent) (20 μl/well) for 3 hr, was evaluated by measuring the optical density (OD) at 490 nm using a Victor X3 Light Plate Reader (PerkinElmer, Waltham, MA).

2.7 | Flow cytometry of apoptotic cells and cell caspase-3/7 activity

H9c2 cells, HL-1 cells, and primary cardiomyocytes were seeded in a 100-mm dish (5×10^5 cells/dish) or 96-well plate (1×10^4 cells/well), respectively. The next day, cells were treated with 0–1 μM Mad for 48 or 24 hr, with six replicates of each treatment. Subsequently, apoptotic cells were monitored by annexin-V–FITC/PI staining and analyzed using a fluorescence-activated cell sorter Vantage SE flow cytometer (Becton Dickinson, San Jose, CA). Caspase-3/7 activity was determined using the Caspase-Glo 3/7 Assay Kit (Promega), following the instructions of the supplier.

2.8 | DAPI and terminal-deoxynucleotidyl-transferase-mediated deoxyuridine triphosphate nick-end labeling staining

H9c2 cells, HL-1 cells, and primary cardiomyocytes, or H9c2 cells infected with Ad-MKK1-R4F, Ad-MKK1-K97M, Ad-PTEN-C/S, Ad-myr-Akt, Ad-PTEN-C/S/Ad-myr-Akt, Ad-myr-Akt/Ad-MKK1-R4F or Ad-GFP, or H9c2 cells infected with lentiviral shRNAs to

Erk1/2 or GFP, respectively, were seeded in a six-well plate (5×10^5 cells/well). Next day, cells were treated with 0–1 μM Mad or with/without 0.5 and 1 μM Mad for 48 hr or treated with/without 0.5 and/or 1 μM Mad for 48 hr after preincubation with/without 5 mM NAC for 1 hr with six replicates of each treatment. Subsequently, the cells with fragmented and condensed nuclei were determined using DAPI staining as described (L. Chen et al., 2008). For the cells pretreated with/without 0–1 μM of Mad for 48 hr, after DAPI staining, terminal-deoxynucleotidyl-transferase-mediated deoxyuridine triphosphate nick-end labeling staining (TUNEL) staining was performed according to the manufacturer's protocols of the In Situ Cell Death Detection Kit (Roche, Mannheim, Germany). For cardiac muscle of Mad-exposed mice, paraffin-embedded cardiac tissue sections were prepared, followed by TUNEL staining, as described (S. Chen et al., 2014). Finally, photographs were taken under a fluorescence microscope (Leica DMi8, Wetzlar, Germany) equipped with a digital camera. For quantitative analysis of the fluorescence intensity using TUNEL staining, the integral OD (IOD) was measured by Image-Pro Plus 6.0 software (Media Cybernetics Inc., Newburyport, MA).

2.9 | Immunofluorescence staining

H9c2 cells, HL-1 cells, and primary cardiomyocytes were seeded at a density of 2×10^5 cells/well in a six-well plate containing a glass coverslip per well. The next day, after treatment with Mad (0–1 μM) for 24 hr, the cells on the coverslips were fixed with 4% paraformaldehyde and incubated with 3% normal goat serum to block nonspecific binding. For cardiac muscle of Mad-exposed mice, paraffin sections were dewaxed using xylene and dehydrated, followed by antigen retrieval, washing with phosphate-buffered saline (PBS), and sealing in 10% bovine serum albumin (BSA), as described (Y. Xu et al., 2014). Next, the cells and tissue sections were incubated with mouse anti-phospho-Erk1/2 antibody (Santa Cruz Biotechnology; 1:50, diluted in PBS containing 1% BSA) overnight at 4°C, washed three times (5 min per time) with PBS, followed by incubating with FITC-conjugated goat antimouse immunoglobulin G (IgG) (Santa Cruz Biotechnology; 1:500, diluted in PBS containing 1% BSA) for 1 hr at room temperature. The cells and tissue sections were then washed three times (5 min per time) with PBS. Finally, the slides for the cells and tissue sections were mounted in glycerol/PBS (1:1, v/v) containing 2.5% 1,4-diazabicyclo-(2,2,2)octane. Cell images were captured under a fluorescence microscope (Leica DMi8) equipped with a digital camera. IOD for fluorescence intensity was quantitatively analyzed by Image-Pro Plus 6.0 software as described above.

2.10 | ROS detection

Detecting intracellular ROS was performed using an oxidant-sensitive probe, CM-H$_2$DCFDA, as described previously (R. Zhang et al., 2017). H9c2 cells, HL-1 cells, and primary cardiomyocytes were seeded in a 96-well plate (1×10^4 cells/well). Next day, cells were treated with 0–1 μM Mad or treated with/without 0.5 and/or 1 μM Mad for 24 hr after preincubation with/without 5 mM NAC for 1 hr

with six replicates of each treatment. Subsequently, cells were loaded with 10 μM CM-H$_2$DCFDA for 40 min. Fluorescent intensity was recorded by excitation at 485 nm and emission at 535 nm using a Victor X3 Light Plate Reader (PerkinElmer).

For heart tissues, the ventricle homogenates were diluted 1:20 (vol/vol) with ice-cold Locke's buffer (154 mM NaCl, 5.6 mM KCl, 3.6 mM NaHCO$_3$, 2.0 mM CaCl$_2$, 10 mM D-glucose, and 5 mM HEPES, pH 7.4) to obtain a concentration of 10 mg tissue/ml. The reaction mixture (1 ml) containing Locke's buffer (pH 7.4), 0.2 ml homogenates, and 10 μl of CM-H$_2$DCFDA (10 μM) was incubated for 15 min at room temperature to allow the CM-H$_2$DCFDA to be incorporated into any membrane-bound vesicles and the diacetate group to be cleaved by esterases. After further incubation for 30 min, the fluorescent intensity for the conversion of CM-H$_2$DCFDA to fluorescent product dichlorofluorescin (DCF) was recorded. Above ROS formation was quantified from a DCF-standard curve, and data were expressed as picomoles (pM) DCF formed/min/mg protein.

2.11 | Western blot analysis

Western blotting was performed, as described previously (X. Chen et al., 2014). Heart tissues were homogenized in 3 ml of ice-cold radioimmunoprecipitation assay (RIPA) buffer. For in vitro H9c2 cells, HL-1 cells, and primary cardiomyocytes, after treatment, cells were briefly washed with cold PBS, and then on ice, lysed in RIPA buffer. Homogenates or lysates were sonicated for 10 s and centrifuged at 14,000 rpm for 10 min at 4°C. After that, the supernatants or lysates containing equivalent amounts of protein were separated on 7–12% sodium dodecyl sulfate-polyacrylamide gel and transferred to polyvinylidene difluoride membranes (Millipore). Membranes were incubated with PBS containing 0.05% Tween 20% and 5% nonfat dry milk to block nonspecific binding and then with primary antibodies against phospho-Akt (p-Akt) (Thr308), p-Akt (Ser473), cleaved-caspase-3, poly (ADP-ribose) polymerase (PARP), glyceraldehyde 3-phosphate dehydrogenase (GAPDH) (Cell Signaling Technology, Danvers, MA), p-Erk1/2 (Thr202/Tyr204), Erk2, Akt (Santa Cruz Biotechnology), p-PTEN (Thr366), PTEN (Epitomics, Burlingame, CA), MKK1, FLAG, HA (Sigma) overnight at 4°C, respectively, followed by incubation with appropriate secondary antibodies, including horse-radish-peroxidase-coupled goat anti-rabbit IgG, goat anti-mouse IgG, or rabbit anti-goat IgG (Pierce, Rockford, IL) overnight at 4°C. Immunoreactive bands were visualized by using enhanced chemiluminescence solution (Millipore).

2.12 | Statistical analysis

Results were expressed as mean values ± standard error. Statistically significant differences between treatment means were identified by using Student's t-test for nonpaired replicates. One-way or two-way analysis of variance followed by Bonferroni's post-tests to compare replicate means was conducted to compare group variability and interaction. A level of $p < 0.05$ was considered to be significant.
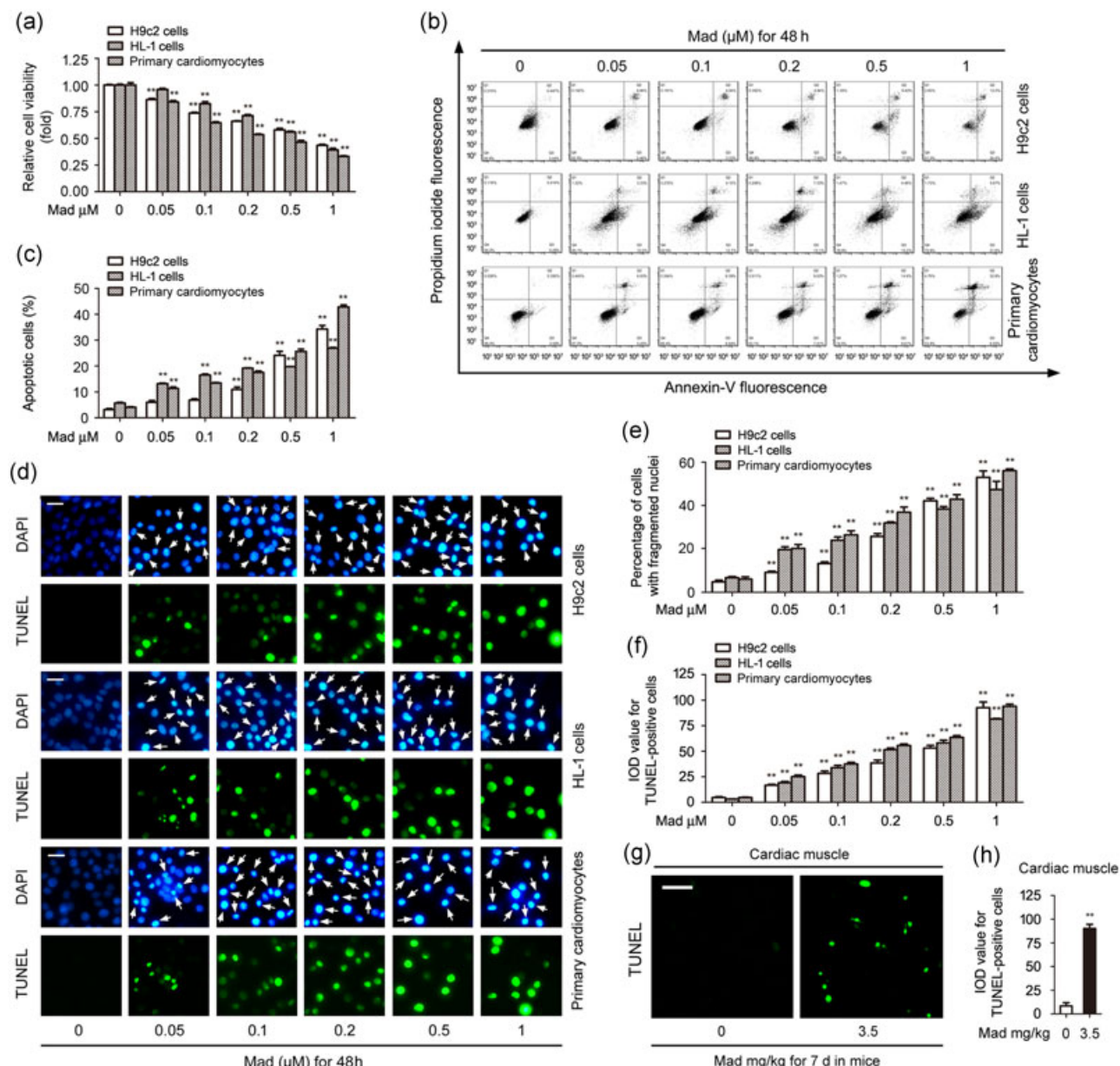
FIGURE 1 Mad evokes apoptotic cell death in cardiac muscle cells and tissues. H9c2, HL-1 cells, and primary cardiomyocytes were treated with Mad (0–1 μM) for 48 hr. The mice were intragastrically administered with Mad (3.5 mg/kg) for 7 days. (a) Cell viability was determined by the MTS assay. (b) The percentages of live (Q4), early apoptotic (Q3), late apoptotic (Q2), and necrotic cells (Q1) were determined by FACS using annexin-V–FITC/PI staining. The results from a representative experiment are shown. (c) Quantitative analysis of apoptotic cells by the FACS assay. (d–h) Cell apoptosis was assayed using DAPI and/or TUNEL staining. The cells with nuclear fragmentation and condensation (arrows) and TUNEL-positive cells (in green) with DNA brand breaks are shown (d, g), respectively, and the quantitative data were indicated (e, f, h). Scale bar= 20 μm. For (a), (c), (e), (f), and (h), all data were expressed as mean ± SE ($n = 6$). **$p < 0.01$, difference with the control group. DAPI: 4′,6-diamidino-2-phenylindole; FACS: fluorescence activated cell sorting; FITC: fluorescein isothiocyanate; Mad: maduramicin; MTS: 3-(4,5-dimethylthiazol-2-yl)-5-(3-carboxymethoxyphenyl)-2-(4-sulfophenyl)-2H-tetrazolium, inner salt; PI: propidium iodide; TUNEL: terminal-deoxynucleotidyl-transferase-mediated deoxyuridine triphosphate nick-end labeling [Color figure can be viewed at wileyonlinelibrary.com]

3 | RESULTS

3.1 | Mad induces apoptotic cell death in cardiac muscle cells

Our previous study has shown that exposure of Mad to C2C12 skeletal muscle cells results in cell viability reduction and identified

that Mad induces apoptosis in the myoblasts (X. Chen et al., 2014). In line with the above findings, here we also observed that treatment with Mad (0–1 μM) for 48 hr resulted in cell viability reduction in cardiac muscle cells (H9c2, HL-1 cells, and primary cardiomyocytes) in a concentration-dependent manner (Figure 1a). To elucidate Mad-induced cardiac apoptosis, annexin-V–FITC/PI staining was used. The

results showed that Mad increased the relative number of apoptotic H9c2, HL-1 cells, and primary cardiomyocytes dose dependently (Figure 1b,c). Mad at $1\,\mu M$ elicited apoptotic cell proportion by 34.33%, 26.89%, and 42.87% compared with the control group in H9c2, HL-1 cells, and primary cardiomyocytes (Figure 1b,c), respectively. In addition, we further tested the cells with nuclear fragmentation and condensation, a hallmark of apoptosis (Hao, Cheng, Clancy, & Nguyen, 2013), using DAPI staining, and concurrently analyzed DNA strand breaks in the cells by TUNEL staining (Figure 1d–f). Imaged and quantified results exhibited that the percentage of the cells with nuclear fragmentation and condensation (arrows) and the number of TUNEL-positive cells with fragmented DNA (in green) increased significantly in H9c2, HL-1 cells, and primary cardiomyocytes induced by 48-hr exposure to Mad,

compared with the control (Figure 1d–f). Similar results were also observed in the cardiac muscle of Mad-exposed mice (3.5 mg/kg) by intragastric administration for 7 days (Figure 1g,h). Collectively, the findings indicate that Mad induces apoptotic cell death in cardiac muscle cells.

3.2 | Mad inhibits the Erk1/2 pathway contributing to apoptosis in cardiac muscle cells

It has been reported that Erk1/2 was involved in the regulation of cell apoptosis (Kyriakis & Avruch, 2012; Xia et al., 2016). Our western blot analysis also showed that Mad dose dependently evoked robust cleavages of caspase-3 and PARP in H9c2, HL-1 cells, and primary cardiomyocytes (Figure 2a). Interestingly, we found
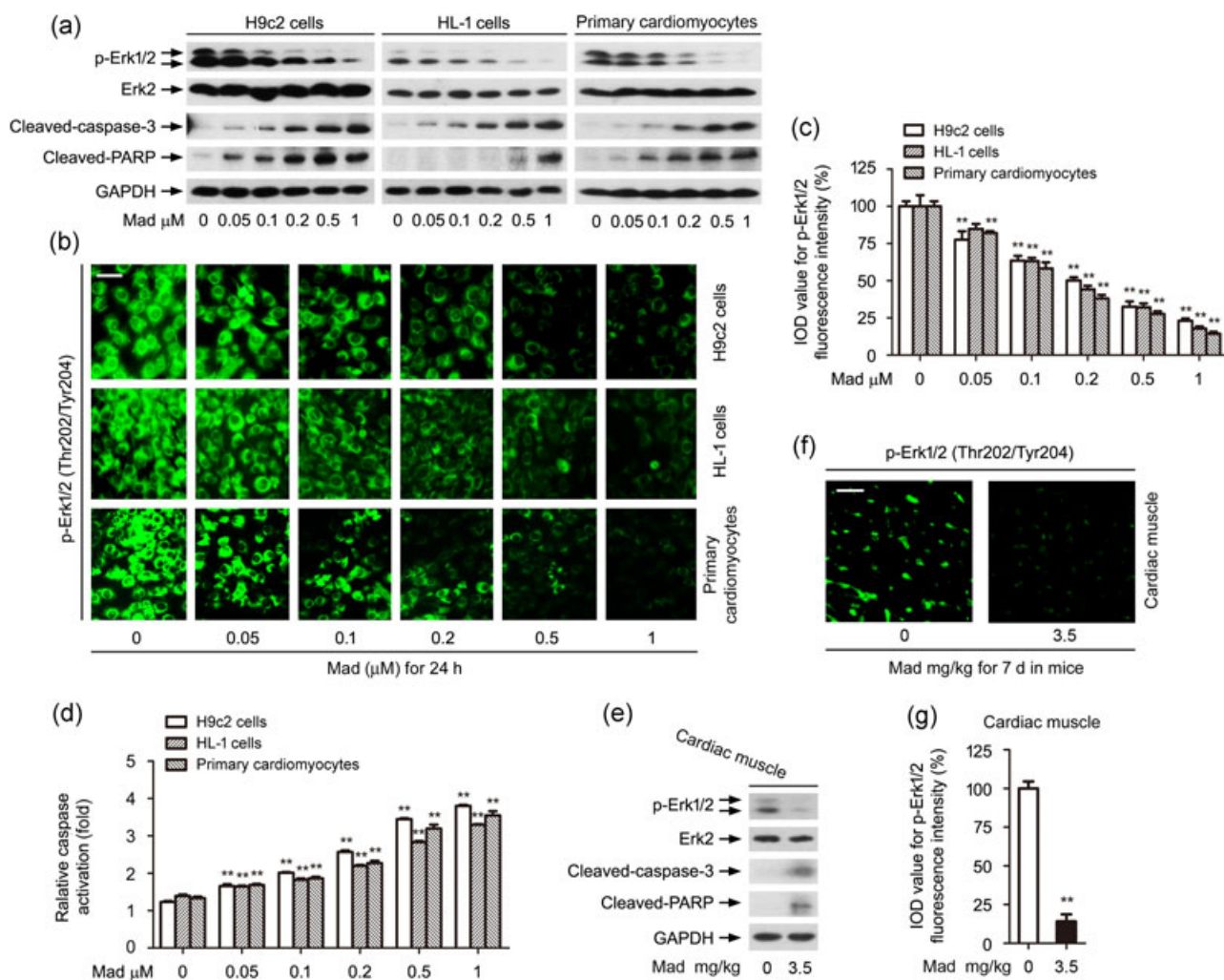
FIGURE 2 Mad induces inactivation of Erk1/2 and activation of caspases in cardiac muscle cells and tissues. H9c2, HL-1 cells, and primary cardiomyocytes were treated with Mad (0–1 μM) for 24 hr. The mice were intragastrically administered with Mad (3.5 mg/kg) for 7 days. (a,e) Total cell lysates and homogenized cardiac muscle supernatants were subjected to western blotting using indicated antibodies. (b,c,f,g) Expression of phospho-Erk1/2 (Thr202/Tyr204) was imaged and quantified using immunofluorescence staining, showing that Mad reduced phospho-Erk1/2 expression (in green) in the cells dose dependently (b,c), and similar findings were seen in cardiac muscles (f,g). Scale bar = 50 μm. (d) Caspase-3/7 activity was determined using caspase-3/7 assay kit, showing that Mad activated caspase-3/7 in the cells. For (a) and (e), the blots were probed for GAPDH as a loading control. Similar results were observed in at least three independent experiments. For (c), (d), and (g), all data were expressed as mean ± SE (n = 6). **p < 0.01, difference with the control group. Erk1/2: extracellular-signal-regulated kinase 1/2; GAPDH: glyceraldehyde 3-phosphate dehydrogenase; Mad: maduramicin; SE: standard error [Color figure can be viewed at wileyonlinelibrary.com]
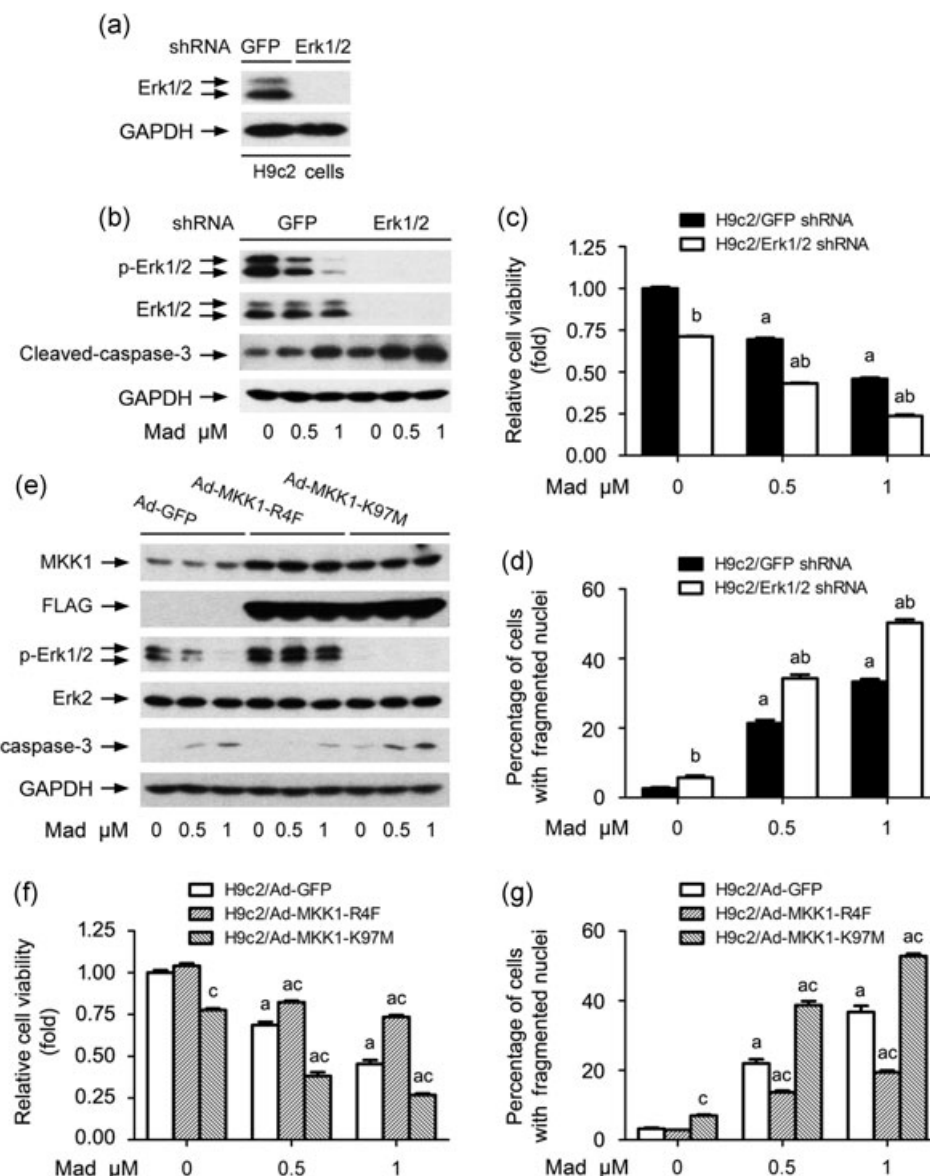
FIGURE 3 Downregulation of Erk1/2 or ectopic expression of MKK1-R4F or MKK1-K97M intervenes in Mad-induced apoptosis in cardiac muscle cells. H9c2 cells, infected with lentiviral shRNA to Erk1/2 or GFP (as control), or with Ad-MKK1-R4F, Ad-MKK1-K97M or Ad-GFP (as control), respectively, were exposed to Mad (0.5 and 1 μM) for 24 hr (for western blotting) or 48 hr (for cell viability assay and cell apoptosis analysis). (a,b,e) Total cell lysates were subjected to Western blotting using indicated antibodies. (c,f) Cell viability was detected by MTS assay. (d,g) Apoptotic cells were evaluated by nuclear fragmentation and condensation using DAPI staining. For (a), (b), and (e), the blots were probed for GAPDH as a loading control. Similar results were observed in at least three independent experiments. For (c), (d), (f), and (g), all data were expressed as mean ± SE ($n = 6$). [a]$p < 0.05$, difference with the control group; [b]$p < 0.05$, Erk1/2 shRNA group versus the GFP shRNA group; [c]$p < 0.05$, Ad-MKK1-R4F group or Ad-MKK1-K97M group versus Ad-GFP group. DAPI: 4′,6-diamidino-2-phenylindole; Erk1/2: extracellular-signal-regulated kinase 1/2; GAPDH: glyceraldehyde 3-phosphate dehydrogenase; GFP: green fluorescence protein; Mad: maduramicin; MTS: 3-(4,5-dimethylthiazol-2-yl)-5-(3-carboxymethoxyphenyl)-2-(4-sulfophenyl)-2H-tetrazolium, inner salt; SE: standard error; shRNA: short hairpin RNA

that Mad reduced phosphorylation of Erk1/2 (Thr202/Tyr204) (Figure 2a), indicating that Mad triggers the inactivation of Erk1/2, which may mediate apoptotic cell death. To confirm this, we further conducted p-Erk1/2 (Thr202/Tyr204) immunofluorescence staining and caspase 3/7 activity assay in the cells, respectively. The results revealed that treatment with Mad (0.05–1 μM) for 24 hr resulted in an obvious decline in the phosphorylation of Erk1/2 (Thr202/Tyr204) (in green) (Figure 2b,c). In line with the Mad-increased cleaved-

caspase-3, Mad profoundly induced the activation of caspases 3/7 in the cells (Figure 2d). Moreover, the events were also observed in murine cardiac muscles exposed to Mad (Figure 2e–g). These data demonstrate that Mad induced inactivation of Erk1/2 and apoptotic cell death in cardiac muscle cells.

To verify the role of Erk1/2 inactivation in Mad-induced apoptosis in cardiac muscle cells, Erk1/2 was silenced by RNA interference. As detected by western blotting, lentiviral shRNA to
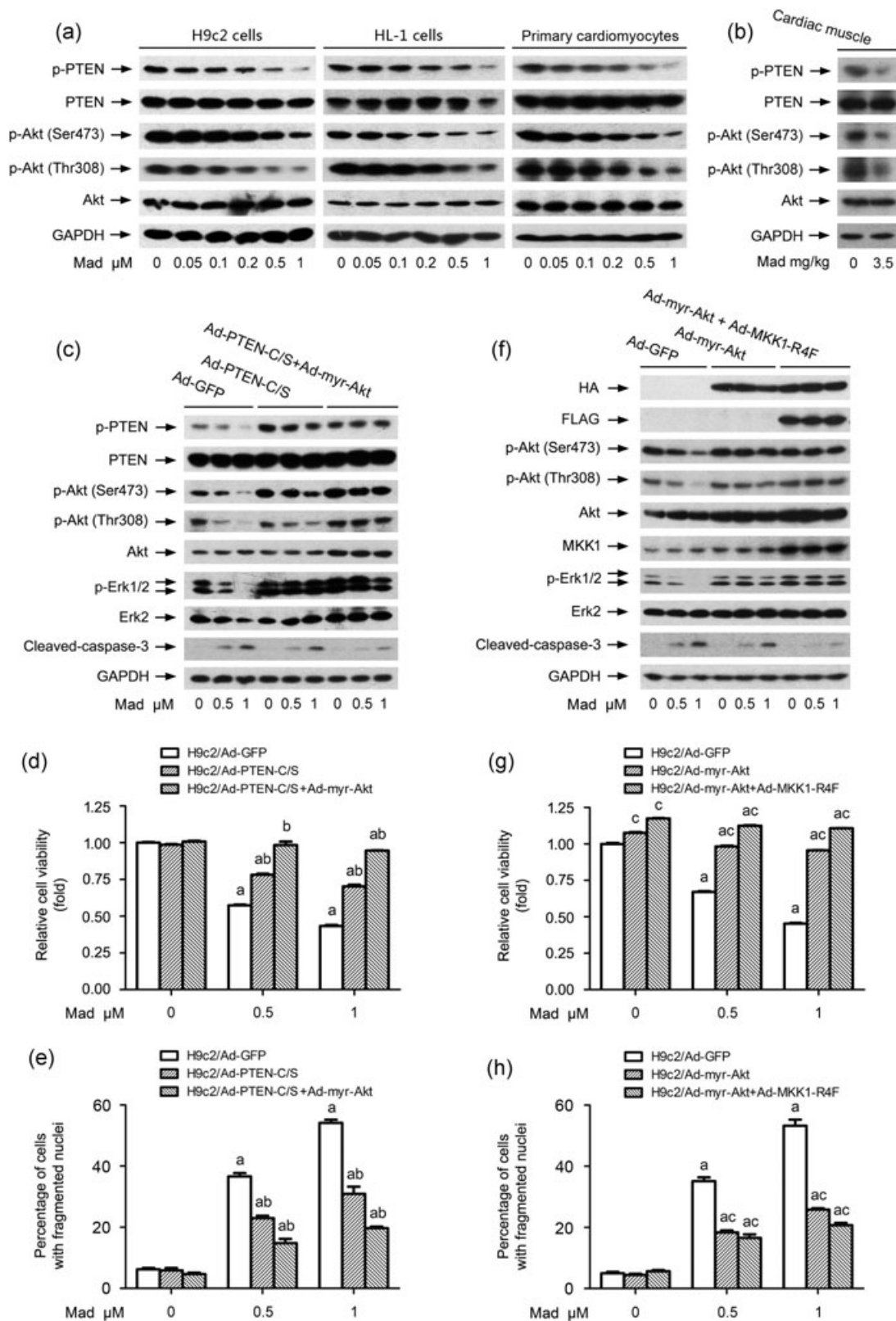
Erk1/2, but not to GFP, downregulated the expression of Erk1/2 by approximately 90% in H9c2 cells (Figure 3a). Silencing Erk1/2 strengthened Mad-induced dephosphorylation of Erk1/2 and cleavage of caspase-3 (Figure 3b). Consistently, downregulation of Erk1/2 enhanced cell viability reduction and apoptosis in H9c2 cells in response to Mad (Figure 3c,d). Furthermore, we extended our studies by modifying MKK1 (an upstream kinase of Erk1/2) activity. To this end, H9c2 cells, infected with recombinant adenoviruses expressing FLAG-tagged constitutively active MKK1 (Ad-MKK1-R4F), dominant negative MKK1 (Ad-MKK1-K97M) and control virus encoding GFP alone (Ad-GFP), respectively, were exposed to Mad (0.5 and 1 μM) for 24 or 48 hr. As expected, expression of high levels of FLAG-tagged MKK1 mutants was seen in Ad-MKK1-R4F- or Ad-MKK1-K97M-infected cells, but not in Ad-GFP-infected cells (control) (Figure 3e). Expression of MKK1-R4F led to robust phosphorylation of Erk1/2 even with exposure to Mad, whereas expression of MKK1-K97M almost completely abolished the basal or Mad-inhibited phosphorylation of Erk1/2 (Figure 3e), indicating that the MKK1 mutants function in the cells. Of note, expression of MKK1-R4F in H9c2 cells conferred profound resistance to Mad-induced cleaved-caspase-3, cell viability reduction, and apoptosis (Figure 3e–g). In contrast, expression of MKK1-K97M in the cells dramatically reinforced the events triggered by Mad (Figure 3e–g). The results clearly indicate that Mad inhibits the Erk1/2 pathway leading to apoptosis in cardiac muscle cells.

3.3 | Mad induces Erk1/2 inhibition and apoptosis in part by activating PTEN and inactivating Akt in cardiac muscle cells

It is well-known that PTEN, Akt, and Erk1/2 interact with each other and regulate cell proliferation/growth and death in a series of cells (Bermudez Brito et al., 2015; Chetram & Hinton, 2012; C. Xu et al., 2015). The current study has found that Mad induces the inactivation of the Erk1/2 pathway (Figures 2 and 3). Therefore, we reasoned that PTEN and/or Akt signaling may be involved in Mad-induced inactivation of Erk1/2, leading to apoptosis in cardiac muscle cells. First, we checked the phosphorylation status of PTEN and Akt in the cells and murine cardiac muscles exposed to Mad. The results showed that Mad inhibited the phosphorylation of PTEN (Thr366) and Akt (Thr308 and Ser473) in H9c2, HL-1 cells, primary

cardiomyocytes dose dependently (Figure 4a). Similar results were observed in murine cardiac muscles (Figure 4b), implying that Mad activates PTEN and inactivates Akt in cardiac muscle cells. Next, H9c2 cells, infected with Ad-PTEN-C/S, Ad-PTEN-C/S/Ad-myr-Akt, and Ad-GFP (as control), respectively, were exposed to Mad (0.5 and 1 μM) for 24 or 48 hr. Infection with Ad-PTEN-C/S and Ad-myr-Akt, but not Ad-GFP, evoked the expression of high levels of p-PTEN and HA-tagged Akt mutant in the cells (Figure 4c). Overexpression of PTEN-C/S in H9c2 cells rendered remarkable resistance to Mad-induced dephosphorylation of Erk1/2 and cleavage of caspase-3 (Figure 4c), as well as cell viability reduction and apoptosis (Figure 4d,e). Of importance, Mad-induced events were more potently ameliorated in Ad-PTEN-C/S/Ad-myr-Akt-infected cells than in Ad-PTEN-C/S- or Ad-GFP-infected cells (Figure 4c–e). Collectively, the findings support the notion that Mad induces suppression of Erk1/2 and consequential cell apoptosis in cardiac muscle cells, in part, by activation of PTEN and inactivation of Akt.

To further uncover the role of Akt in Mad-induced Erk1/2 inactivation and apoptosis in cardiac muscle cells, H9c2 cells infected with Ad-myr-Akt and/or Ad-MKK1-R4F were utilized. As shown in Figure 4f, expression of high levels of HA-tagged Akt and/or FLAG-tagged MKK1 mutants was seen in H9c2 cells infected with Ad-myr-Akt and/or Ad-MKK1-R4F, but not in the cells infected with Ad-GFP (control virus). Overexpression of myr-Akt remarkably prevented Mad-induced dephosphorylation of Akt and Erk1/2, cleaved-caspase-3, cell viability reduction, and apoptosis (Figure 4f–h). Interestingly, the cells expressing myr-Akt/MKK1-R4F possessed more powerful inhibitory effects on Mad-induced events than the cells expressing myr-Akt alone (Figure 4f–h). These data indicate that Mad elicited Erk1/2 inhibition contributing to apoptosis partly by the inactivation of Akt in cardiac muscle cells.

3.4 | Mad-induced ROS results in PTEN activation and Akt–Erk1/2 inactivation, leading to apoptosis in cardiac muscle cells

ROS has been identified as a key player in cardiomyocyte apoptosis (Lv et al., 2014; Matsuno et al., 2012; Tian et al., 2012; Yao et al., 2016). To unveil whether Mad induces ROS in cardiac muscle cells, H9c2, HL-1 cells, and primary cardiomyocytes were

FIGURE 4 PTEN–Akt pathway is involved in Mad-induced Erk1/2-dependent apoptosis in cardiac muscle cells and tissues. H9c2, HL-1 cells, and primary cardiomyocytes, or H9c2 cells infected with Ad-GFP (as control), Ad-PTEN-C/S, Ad-myr-Akt, and/or Ad-MKK1-R4F were treated with Mad (0–1 μM, or 0.5 and 1 μM) for 24 hr (for western blotting) or 48 hr (for cell viability assay and cell apoptosis analysis). The mice were intragastrically administered with Mad (3.5 mg/kg) for 7 days. (a,b,c,f) Total cell lysates and homogenized cardiac muscle supernatants were subjected to western blotting using indicated antibodies. (d, g) Cell viability was detected by MTS assay. (e, h) Apoptotic cells were evaluated by nuclear fragmentation and condensation using DAPI staining. For (a), (b), (c), and (f), the blots were probed for GAPDH as a loading control. Similar results were observed in at least three independent experiments. For (d), (e), (g), and (h), all data were expressed as mean ± SE (n = 6). [a]p < 0.05, difference with the control group; [b]p < 0.05, Ad-PTEN-C/S and/or Ad-myr-Akt group versus the Ad-GFP group; [c]P < 0.05, Ad-myr-Akt and/or Ad-MKK1-R4F group versus Ad-GFP group. Ad-GFP: adenoviruses expressing green fluorescence protein; Akt: protein kinase B; DAPI: 4′,6-diamidino-2-phenylindole; Erk1/2: extracellular-signal-regulated kinase 1/2; GAPDH: glyceraldehyde 3-phosphate dehydrogenase; Mad: maduramicin; MTS: 3-(4, 5-dimethylthiazol-2-yl)-5-(3-carboxymethoxyphenyl)-2-(4-sulfophenyl)-2H-tetrazolium, inner salt; PTEN: phosphatase and tensin homolog on chromosome 10; SE: standard error
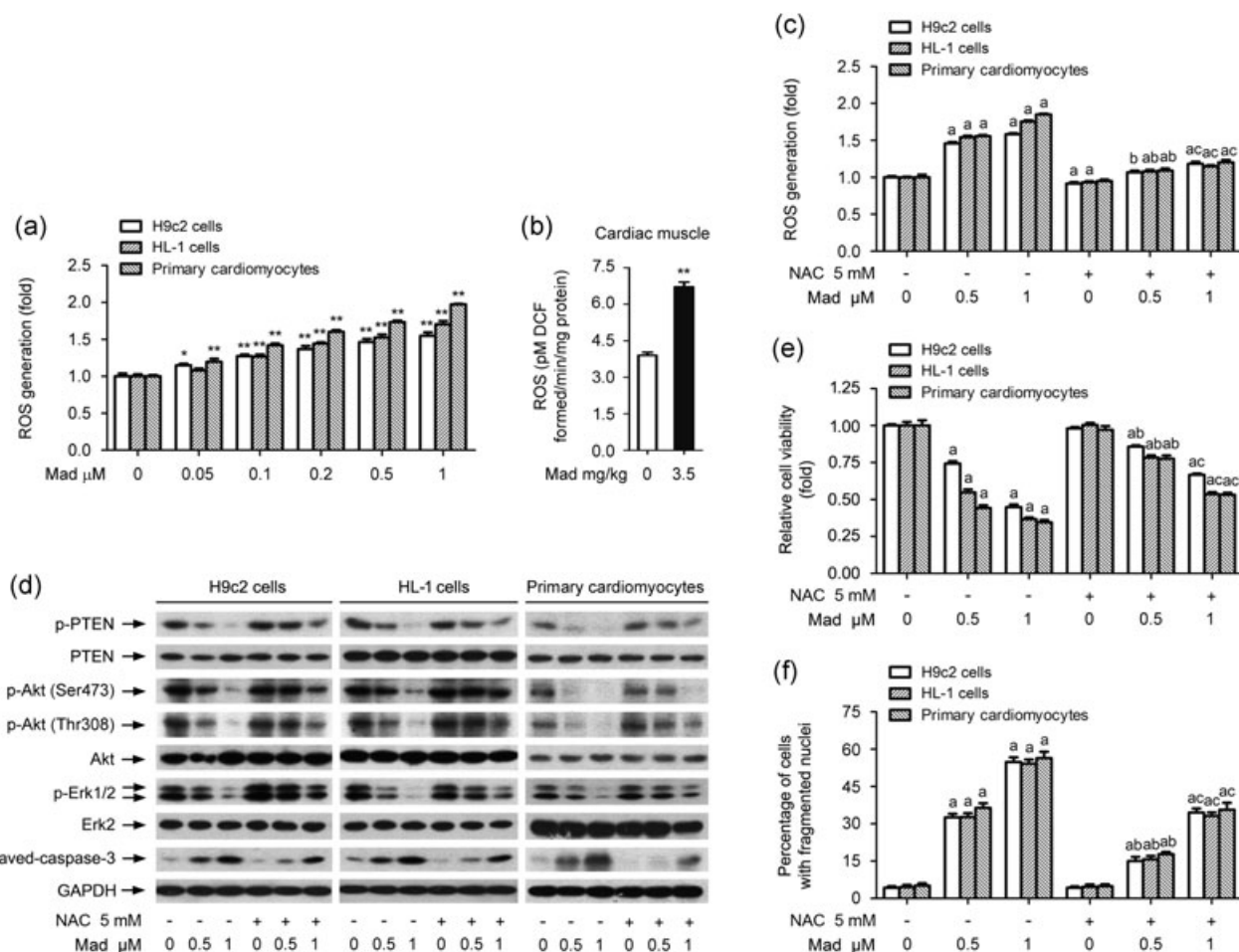
FIGURE 5 Mad induces apoptosis by triggering ROS-dependent activation of PTEN and inactivation Akt–Erk1/2 in cardiac muscle cells and tissues. H9c2, HL-1 cells, and primary cardiomyocytes were exposed to Mad (0–1 μM) for 24 hr or pretreated with/without NAC (5 mM) for 1 hr and then exposed to Mad (0.5 and 1 μM) for 24 hr (for ROS detection and western blotting) or 48 hr (for cell viability assay and cell apoptosis analysis). The mice were intragastrically administered with Mad (3.5 mg/kg) for 7 days. (a–c) ROS level was detected using an oxidant-sensitive probe CM-H$_2$DCFDA. (d) Total cell lysates were subjected to western blotting using indicated antibodies. (e) Cell viability was detected by the MTS assay. (f) Apoptotic cells were evaluated by nuclear fragmentation and condensation using DAPI staining. For (d), the blots were probed for GAPDH as a loading control. Similar results were observed in at least three independent experiments. For (a), (b), (c), (e), and (f), all data were expressed as mean ± SE ($n = 6$). $^*p < 0.05$, $^{**}p < 0.01$, $^ap < 0.05$, difference with control group; $^bp < 0.05$, difference with 0.5 μM Mad group; $^cp < 0.05$, difference with 1 μM Mad group. Akt: protein kinase B; CM-H$_2$DCFDA: 5-(and-6)-chloromethyl-2',7'-dichlorodihydrofluorescein diacetate; DAPI: 4',6-diamidino-2-phenylindole; Erk1/2: extracellular-signal-regulated kinase 1/2; GAPDH: glyceraldehyde 3-phosphate dehydrogenase; Mad: maduramicin; MTS: 3-(4,5-dimethylthiazol-2-yl)-5-(3-carboxymethoxyphenyl)-2-(4-sulfophenyl)-2H-tetrazolium, inner salt; NAC: N-acetyl-L-cysteine; PTEN: phosphatase and tensin homolog on chromosome 10; ROS: reactive oxygen species; SE: standard error

treated with Mad (0–1 μM) for 24 hr, or mice were intragastrically administered with Mad (3.5 mg/kg) for 7 days, followed by ROS detection using CM-H$_2$DCFDA. As shown in Figure 5a,b, Mad treatment significantly increased the ROS levels in the cells and cardiac muscles, which was markedly attenuated by pretreatment with NAC, an antioxidant and ROS scavenger (Figure 5c). NAC also attenuated the effects of Mad on the expression of p-PTEN, p-Akt, and p-Erk1/2 in the cells (Figure 5d). Importantly, Mad-induced cleaved-caspase-3, cell viability reduction, and apoptosis were substantially weakened by pretreatment with NAC (Figure 5d–f). These results clearly indicate that Mad-elevated ROS activates PTEN and inactivates Akt–Erk1/2, thereby leading to apoptosis in cardiac muscle cells.

4 | DISCUSSION

Mad, an anticoccidial agent used in the poultry, has been reported to be toxic to the humans and animals, such as chickens, turkeys, pigs, cattle, sheep, and so forth (Bastianello et al., 1995; Dorne et al., 2013; Fourie et al., 1991; Jayashree & Singhi, 2011; Shimshoni et al., 2014). Especially, emerging studies have pointed out Mad-induced severe myocardial and skeletal muscle lesions (Bastianello et al., 1995; Dorne et al., 2013; Fourie et al., 1991; Jayashree & Singhi, 2011; Shimshoni et al., 2014). Of importance, growing reports have documented the human cases of poisoning with Mad by accident (Jayashree & Singhi, 2011; Sharma et al., 2005). Our recent study has shown that Mad inhibits proliferation and induces apoptosis in

C2C12 skeletal muscle cells (X. Chen et al., 2014). However, little is known about the toxic mechanism of Mad in cardiac muscle cells. Here, we provide evidence that Mad induced apoptotic cell death by inhibiting the Erk1/2 pathway in cardiac muscle cells. Furthermore, we found that Mad induction of intracellular ROS elicited inhibition of Erk1/2 contributing to cell apoptosis via activation of PTEN and inactivation of Akt.

In this study, we found that Mad induced dephosphorylation of Erk1/2 and cleavages of caspase-3 and PARP in H9c2, HL-1 cells, primary cardiomyocytes, and murine cardiac muscle, as detected by western blotting (Figure 2a,e). This is further supported by the results of phospho-Erk1/2 immunofluorescence staining and caspase 3/7 activity assay (Figure 2b–d,f,g). To corroborate the above findings, genetic inhibition/silencing, or rescue experiments for Erk1/2 was carried out. We showed that silencing Erk1/2 strengthened Mad-induced dephosphorylation of Erk1/2 and cleavage of caspase-3 (Figure 3b). Concurrently, silencing Erk1/2 conferred substantial enhancement of Mad-induced apoptotic cell death, as evidenced by more reduced cell viability and elevated percentages of cells with nuclear fragmentation and condensation in H9c2 cells (Figure 3c,d). Furthermore, we found that ectopic expression of dominant negative MKK1 (MKK-K97M) strengthened Mad-induced dephosphorylation of Erk1/2, cleaved-caspase-3, and cell apoptosis, whereas expression of constitutively active MKK1 (MKK1-R4F) attenuated these events in H9c2 cells (Figure 3e–g). Taken together, these observations support that Mad induces apoptotic cell death, at least in part, by the inactivation of the Erk1/2 pathway in cardiac muscle cells.

It is well-known that PTEN negatively regulates Akt signaling (Maehama & Dixon, 1999; Panigrahi et al., 2004). In this study, we observed that Mad upregulated PTEN activity and inhibited Akt, as Mad reduced the phosphorylation levels of PTEN and Akt in H9c2, HL-1 cells, primary cardiomyocytes, and mice cardiac muscle (Figure 4a,b). Recent studies have suggested that PTEN also negatively regulates the Erk1/2 pathway in several malignancies (Chetram & Hinton, 2012). In addition, Akt is able to activate Erk1/2 through PKC (Chetram & Hinton, 2012). Putting all data together, we postulated that there may exist a cross-talk between PTEN, Akt, and Erk1/2 pathways in cardiac muscle cells in response to Mad, that is, Mad upregulation of PTEN and concurrent inhibition of Akt may cause inactivation of Erk1/2. Here, for the first time, we present evidence that Mad induced cardiac apoptosis indeed by upregulation of PTEN and inactivation of Akt, resulting in inhibition of the Erk1/2 pathway. This is strongly supported by the findings that ectopic expression of dominant negative PTEN (PTEN-C/S) and/or myr-Akt, or myr-Akt and/or constitutively active MKK1 (MKK1-R4F) dramatically rescued the cells from Mad-induced dephosphorylated-Erk1/2 and cell death in H9c2 cells (Figure 4c–h). Our data underscore that Mad induces activation of PTEN and inactivation of Akt, also contributing to Erk1/2 inhibition, and eventually apoptosis in cardiac muscle cells.

A new question that arises from this work is how Mad activates PTEN signaling and, thus, inhibits the Akt–Erk1/2 pathway, leading to apoptosis in cardiac muscle cells. Many studies have shown that ROS can alter the structures and functions of cellular proteins and also
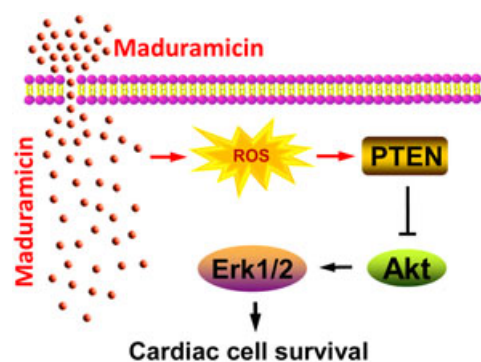
FIGURE 6 A schematic model of how Mad inhibits Erk1/2, leading to cardiomyocyte apoptosis. Mechanistically, Mad induction of ROS inhibits Erk1/2 leading to apoptosis by upregulation of PTEN and inactivation of Akt in cardiac muscle cells. Akt: protein kinase B; Erk1/2: extracellular-signal-regulated kinase 1/2; Mad: maduramicin; PTEN: phosphatase and tensin homolog on chromosome 10; ROS: reactive oxygen species [Color figure can be viewed at wileyonlinelibrary.com]

activate or inhibit related signaling pathways, leading to cardiomyocyte apoptosis (Lv et al., 2014; Matsuno et al., 2012; Tian et al., 2012; Yao et al., 2016). It has been reported that the polyether ionophore, such as salinomycin, induces intracellular ROS overproduction (Verdoodt et al., 2012; Zhou et al., 2013). Excessive ROS-induced cardiomyocyte apoptosis links to dysfunction of PTEN, Akt, and/or Erk1/2 signaling (Kim et al., 2014; Lv et al., 2014; Matsuno et al., 2012; Tian et al., 2012; Yao et al., 2012; Yao et al., 2016). During our research, we also observed that when H9c2, HL-1 cells, and primary cardiomyocytes were exposed to Mad (0.05–1 μM) for 24 hr, or mice were intragastrically administered with Mad (3.5 mg/kg) for 7 days, cellular ROS level was significantly elevated compared with the vehicle-treated cells or murine cardiac muscles (Figure 5a,b). Pretreatment with NAC not only scavenged Mad-induced cellular ROS but also reversed Mad-elicited activation of PTEN and inactivation of Akt–Erk1/2, as well as apoptosis in the cells (Figure 5c–f). Taken together, we conclude that Mad acts by the mechanism that activates PTEN and inactivates Akt, and consequently inhibits the Erk1/2 pathway leading to cardiac apoptosis through induction of ROS generation. Mad may be involved in interactions of diverse signals and expression of genes associated with cardiotoxicity. Undoubtedly, more studies are needed to address this issue.

In summary, here we have demonstrated that Mad induction of ROS inhibits Erk1/2 leading to apoptosis through upregulation of PTEN and inactivation of Akt in cardiac muscle cells (Figure 6). The results indicate that Mad induces cardiac apoptosis, at least in part, through targeting ROS-dependent PTEN–Akt–Erk1/2 signaling network. Our findings suggest that manipulation of the ROS–PTEN–Akt–Erk1/2 pathway may be a potential approach for the prevention of Mad-induced cardiotoxicity.

ORCID

Shile Huang (iD) http://orcid.org/0000-0002-3239-1072
Long Chen (iD) http://orcid.org/0000-0002-2050-8050

REFERENCES

Bastianello, S. S., Fourie, N., Prozesky, L., Nel, P. W., & Kellermann, T. S. (1995). Cardiomyopathy of ruminants induced by the litter of poultry fed on rations containing the ionophore antibiotic, maduramicin. II. Macropathology and histopathology. *Onderstepoort Journal of Veterinary Research*, 62(1), 5–18.

Bermúdez brito, M., Goulielmaki, E., & Papakonstanti, E. A. (2015). Focus on PTEN regulation. *Frontiers in Oncology*, 5, 166.

Chen, L., Liu, L., Luo, Y., & Huang, S. (2008). MAPK and mTOR pathways are involved in cadmium-induced neuronal apoptosis. *Journal of Neurochemistry*, 105(1), 251–261.

Chen, S., Ren, Q., Zhang, J., Ye, Y., Zhang, Z., Xu, Y., ... Chen, L. (2014). N-acetyl-L-cysteine protects against cadmium-induced neuronal apoptosis by inhibiting ROS-dependent activation of Akt/mTOR pathway in mouse brain. *Neuropathology and Applied Neurobiology*, 40(6), 759–777.

Chen, X., Gu, Y., Singh, K., Shang, C., Barzegar, M., Jiang, S., & Huang, S. (2014). Maduramicin inhibits proliferation and induces apoptosis in myoblast cells. *PLoS One*, 9(12), e115652.

Chetram, M. A., & Hinton, C. V. (2012). PTEN regulation of ERK1/2 signaling in cancer. *Journal of Receptor and Signal Transduction Research*, 32(4), 190–195.

Dorne, J. L., Fernández-Cruz, M. L., Bertelsen, U., Renshaw, D. W., Peltonen, K., Anadon, A., ... Fink-Gremmels, J. (2013). Risk assessment of coccidostatics during feed cross-contamination: Animal and human health aspects. *Toxicology and Applied Pharmacology*, 270(3), 196–208.

Findley, C. M., Cudmore, M. J., Ahmed, A., & Kontos, C. D. (2007). VEGF induces Tie2 shedding via a phosphoinositide 3-kinase/Akt dependent pathway to modulate Tie2 signaling. *Arteriosclerosis, Thrombosis, and Vascular Biology*, 27(12), 2619–2626.

Fourie, N., Bastianello, S. S., Prozesky, L., Nel, P. W., & Kellerman, T. S. (1991). Cardiomyopathy of ruminants induced by the litter of poultry fed on rations containing the ionophore antibiotic, maduramicin. I. Epidemiology, clinical signs and clinical pathology. *Onderstepoort Journal of Veterinary Research*, 58(4), 291–296.

Fujio, Y., & Walsh, K. (1999). Akt mediates cytoprotection of endothelial cells by vascular endothelial growth factor in an anchorage-dependent manner. *The Journal of Biological Chemistry*, 274(23), 16349–16354.

Hao, B., Cheng, S., Clancy, C. J., & Nguyen, M. H. (2013). Caspofungin kills *Candida albicans* by causing both cellular apoptosis and necrosis. *Antimicrobial Agents and Chemotherapy*, 57(1), 326–332.

Jayashree, M., & Singhi, S. (2011). Changing trends and predictors of outcome in patients with acute poisoning admitted to the intensive care. *Journal of Tropical Pediatrics*, 57(5), 340–346.

Kim, D. E., Kim, B., Shin, H. S., Kwon, H. J., & Park, E. S. (2014). The protective effect of hispidin against hydrogen peroxide-induced apoptosis in H9c2 cardiomyoblast cells through Akt/GSK-3beta and ERK1/2 signaling pathway. *Experimental Cell Research*, 327(2), 264–275.

Kyriakis, J. M., & Avruch, J. (2012). Mammalian MAPK signal transduction pathways activated by stress and inflammation: A 10-year update. *Physiological Reviews*, 92(2), 689–737.

Liu, J., Mao, W., Ding, B., & Liang, C. (2008). ERKs/p53 signal transduction pathway is involved in doxorubicin-induced apoptosis in H9c2 cells and cardiomyocytes. *American Journal of Physiology: Heart and Circulatory Physiology*, 295(5), H1956–H1965.

Lv, G., Shao, S., Dong, H., Bian, X., Yang, X., & Dong, S. (2014). MicroRNA-214 protects cardiac myocytes against H2O2-induced injury. *Journal of Cellular Biochemistry*, 115(1), 93–101.

Maehama, T., & Dixon, J. E. (1999). PTEN: A tumour suppressor that functions as a phospholipid phosphatase. *Trends in Cell Biology*, 9(4), 125–128.

Matsuno, K., Iwata, K., Matsumoto, M., Katsuyama, M., Cui, W., Murata, A., ... Yabe-Nishimura, C. (2012). NOX1/NADPH oxidase is involved in endotoxin-induced cardiomyocyte apoptosis. *Free Radical Biology and Medicine*, 53(9), 1718–1728.

Panigrahi, A., Pinder, S., Chan, S., Paish, E., Robertson, J., & Ellis, I. (2004). The role of PTEN and its signalling pathways, including AKT, in breast cancer; an assessment of relationships with other prognostic factors and with outcome. *Journal of Pathology*, 204(1), 93–100.

Park, W., Kim, E., Kim, B., & Lee, Y. (2003). Monensin-mediated growth inhibition in NCI-H929 myeloma cells via cell cycle arrest and apoptosis. *International Journal of Oncology*, 23(1), 197–204.

Sanford, S. E., & McNaughton, C. (1991). Ontario. Inonophore (maduramicin) toxicity in pigs. *The Canadian Veterinary Journal*, 32(9), 567.

Sharma, N., Bhalla, A., Varma, S., Jain, S., & Singh, S. (2005). Toxicity of maduramicin. *Emergency Medicine Journal*, 22(12), 880–882.

Shimshoni, J. A., Britzi, M., Pozzi, P. S., Edery, N., Berkowitz, A., Bouznach, A., ... Perl, S. (2014). Acute maduramicin toxicosis in pregnant gilts. *Food and Chemical Toxicology*, 68, 283–289.

Shlosberg, A., Harmelin, A., Perl, S., Pano, G., Davidson, M., Orgad, U., ... Bogin, E. (1992). Cardiomyopathy in cattle induced by residues of the coccidiostat maduramicin in poultry litter given as a feedstuff. *Veterinary Research Communications*, 16(1), 45–58.

Shlosberg, A., Perl, S., Harmelin, A., Hanji, V., Bellaiche, M., Bogin, E., ... Aharoni, Y. (1997). Acute maduramicin toxicity in calves. *The Veterinary Record*, 140(25), 643–646.

Singh, T., & Gupta, R. P. (2003). Clinico-haematological and mineral studies on experimental maduramicin toxicity in chickens. *Veterinary Parasitology*, 116(4), 345–353.

Sun, X. L., Yuan, J., Jin, T., Cheng, X. Q., Wang, Q., Guo, J., ... Zhang, Z. (2017). Physical and functional interaction of Snapin with Cav1.3 calcium channel impacts channel protein trafficking in atrial myocytes. *Cellular Signalling*, 30, 118–129.

Tian, Y., Daoud, A., & Shang, J. (2012). Effects of bpV(pic) and bpV(phen) on H9c2 cardiomyoblasts during both hypoxia/reoxygenation and H2O2-induced injuries. *Molecular Medicine Reports*, 5(3), 852–858.

Ulm, S., Liu, W., Zi, M., Tsui, H., Chowdhury, S. K., Endo, S., ... Wang, X. (2014). Targeted deletion of ERK2 in cardiomyocytes attenuates hypertrophic response but provokes pathological stress induced cardiac dysfunction. *Journal of Molecular and Cellular Cardiology*, 72, 104–116.

Verdoodt, B., Vogt, M., Schmitz, I., Liffers, S. T., Tannapfel, A., & Mirmohammadsadegh, A. (2012). Salinomycin induces autophagy in colon and breast cancer cells with concomitant generation of reactive oxygen species. *PLoS One*, 7(9), e44132.

Xia, P., Liu, Y., & Cheng, Z. (2016). Signaling pathways in cardiac myocyte apoptosis. *BioMed Research International*, 2016, 9583268–22.

Xu, C., Zhang, H., Liu, C., Zhu, Y., Wang, X., Gao, W., … Chen, L. (2015). Rapamycin inhibits Erk1/2-mediated neuronal apoptosis caused by cadmium. *Oncotarget*, *6*(25), 21452–21467.

Xu, Y., Liu, C., Chen, S., Ye, Y., Guo, M., Ren, Q., … Chen, L. (2014). Activation of AMPK and inactivation of Akt result in suppression of mTOR-mediated S6K1 and 4E-BP1 pathways leading to neuronal cell death in in vitro models of Parkinson's disease. *Cellular Signalling*, *26*(8), 1680–1689.

Yao, H., Shang, Z., Wang, P., Li, S., Zhang, Q., Tian, H., … Han, X. (2016). Protection of luteolin-7-O-glucoside against doxorubicin-induced injury through PTEN/Akt and ERK pathway in H9c2 cells. *Cardiovascular Toxicology*, *16*(2), 101–110.

Yao, Y., Li, R., Ma, Y., Wang, X., Li, C., Zhang, X., … Liu, L. (2012). α-Lipoic acid increases tolerance of cardiomyoblasts to glucose/glucose oxidase-induced injury via ROS-dependent ERK1/2 activation. *Biochimica et Biophysica Acta/General Subjects*, *1823*(4), 920–929.

Zhang, D., Zhu, L., Li, C., Mu, J., Fu, Y., Zhu, Q., … Han, C. (2015). Sialyltransferase7A, a Klf4-responsive gene, promotes cardiomyocyte apoptosis during myocardial infarction. *Basic Research in Cardiology*, *110*(3), 28.

Zhang, R., Zhang, N., Zhang, H., Liu, C., Dong, X., Wang, X., … Chen, L. (2017). Celastrol prevents cadmium-induced neuronal cell death by blocking reactive oxygen species-mediated mammalian target of rapamycin pathway. *British Journal of Pharmacology*, *174*(1), 82–100.

Zhang, W., St Clair, D., Butterfield, A., & Vore, M. (2016). Loss of Mrp1 potentiates doxorubicin-induced cytotoxicity in neonatal mouse cardiomyocytes and cardiac fibroblasts. *Toxicological Sciences*, *151*(1), 44–56.

Zhou, J., Li, P., Xue, X., He, S., Kuang, Y., Zhao, H., … Guo, X. (2013). Salinomycin induces apoptosis in cisplatin-resistant colorectal cancer cells by accumulation of reactive oxygen species. *Toxicology Letters*, *222*(2), 139–145.

How to cite this article: Chen X, Li Y, Feng M, et al. Maduramicin induces cardiac muscle cell death by the ROS-dependent PTEN/Akt-Erk1/2 signaling pathway. *J Cell Physiol.* 2019;234:10964–10976. https://doi.org/10.1002/jcp.27830